Temperature Behavior of Visible and Infrared Electroluminescent Devices Fabricated on Erbium-Doped GaN

Michael J. Garter and Andrew J. Steckl, *Fellow, IEEE*

***Abstract*—Visible and infrared (IR) rare-earth-activated light emission has been obtained from Er-doped GaN electroluminescent devices (ELD). The ELD consists of an in-situ Er-doped GaN layer grown on either a sapphire or silicon (Si) substrate. The temperature dependence of the light emission and the current conduction is reported. The EL spectrum shows two main visible peaks at 537 and 558 nm and a group of closely spaced IR peaks clustered around 1550 nm. The 558 nm visible transition is dominant below 250 K, whereas the 537 nm transition is dominant at higher temperature peaking at 300 K. Temperatures from 240–500 K have minimal effect on IR emission intensity. A simple model consisting of two back-to-back Schottky diodes explains the current-voltage dependence. The effect of Er doping and substrate type on carrier transport is investigated as a function of voltage and temperature. Specifically, there is evidence that an Er-related defect is responsible for carrier generation at temperatures above 300 K. The effect of bias polarity on spatial confinement of the light emission in different areas of the devices is discussed. The model indicates that both electric field intensity and current density are important in producing light emission. The model also accounts for the uniformity of the emission under the electrodes when considering the type of substrate used for GaN:Er device growth.**

***Index Terms*—Electroluminescence, Er, GaN, ITO, temperature dependence.**

I. Introduction

RARE-EARTH doped materials have been researched extensively for light emission applications over the past 30 years. Applications include fiber amplifiers, such as erbium doped glass fiber amplifiers, lasers (such as YAG:Nd), and thin film electroluminescent devices (TFELD). Specifically, the ZnSeS system has been used as a host for rare-earth atoms and rare-earth based molecules in order to obtain luminescence. This research has shown that the dominant mechanism of electroluminescence is by carrier impact excitation [1]–[3].

Research on silicon doped with erbium has shown that the infrared (IR) radiation at 1.5 μm, due to an electronic transition from $^4I_{13/2}$ to $^4I_{15/2}$, is generally quenched at temperatures around 300 K [4], [5]. The addition of oxygen has been shown to improve the temperature quenching in silicon [6], [7]. Indeed Si:Er research has shown that practical devices may be possible by overcoming limits on erbium concentration and by changing the local environment of the erbium atoms [8]. GaP has a larger bandgap, which has been shown to improve temperature quenching. However, EL intensity still falls off around 300 K, similar to Si [9]. More recently, rare-earth doped GaN has received attention due to the observation that temperature quenching of the IR radiation is reduced as the band gap of the host semiconductor material increases [10]. In fact, the IR radiation has been investigated using photo-, cathodo-, and electroluminescence studies [11]. The temperature dependence of IR radiation from erbium implanted GaN has also been investigated [12], [13]. In addition, the excitation mechanisms resulting in IR radiation have been investigated [14]. Er-doped GaN was the first III-V semiconductor host to exhibit [15] visible (green) emission at 537 and 558 nm due to electronic transitions from the $^2H_{11/2}$ and $^4S_{3/2}$ to the $^4I_{15/2}$, respectively. Similar to IR emission, the green light emission was observed using photo- [15], [16] , cathodo- [17], and electroluminescence [18]–[20]. Until now, there have been no reports concerning the temperature dependence of the EL intensity (IR or visible light) or current transport mechanisms for GaN:Er. We feel that this information will help clarify the practicality of rare-earth doped GaN EL devices as visible and IR light emitters, especially since our results indicate that temperature quenching of the 1.5 μm radiation in GaN:Er does not occur until higher temperature.

II. Experimental Conditions

A p-type (10 Ω-cm) Si and c-plane sapphire were used as substrates for the GaN:Er ELD structure. The GaN growth was perfomed by MBE in a Riber 32 system.The MBE process starts with the growth of a thin, low temperature GaN buffer layer followed by two GaN layers: $\sim$ 0.6 μm of undoped GaN and $\sim$ 0.6 μm of Er-doped GaN. Finally, a 0.2 μm "capping" layer of undoped GaN was grown. The GaN layers were grown at a substrate temperature of $\sim$700 °C depending on whether a Si or sapphire substrate was used. In general, the reflection high-electron energy diffraction (RHEED) patterns obtained from the erbium doped GaN films during growth were essentially the same for sapphire and silicon substrates. The RHEED patterns were partially spotty and partially streaky. This is due to the use of a slightly Ga deficient growth regime, which enhances the luminescence efficiency of the Er^{3+} ions. Additional information on the growth process of Er-doped GaN can be found elsewhere [21], [22]. A layer of indium tin oxide (ITO) was used to obtain transparent electrodes to the ELD structure. The

Manuscript received May 1, 2001; revised September 4, 2001. This work was supported in part by ARO Contract DAAD19-99-1-038. The review of this paper was arranged by Editor P. Bhattacharya.

The authors are with the Nanoelectronics Laboratory, University of Cincinnati, Cincinnati, OH 45221-0030 USA (e-mail: a.steckl@uc.edu).

Publisher Item Identifier S 0018-9383(02)00234-4.

electrodes were deposited by RF-sputtering from an ITO target with a composition of 90% In_2O_3 and 10% SnO_2 and were patterned with a lift-off process. The sputtering was performed at 5 mtorr with 50 W of RF power, resulting in -123 V of dc bias. Under these conditions, the deposition rate was $\sim$ 40 Å/min. The ITO film was $\sim$ 800 Å thick and had a sheet resistance of 3000 $\Omega/\square$ as-deposited. Postdeposition annealing was performed in an AG Associates rapid thermal annealer at 450 °C for two minutes in a nitrogen atmosphere, resulting in a much reduced sheet resistance of 90 $\Omega/\square$ The ITO film had a transmission of $\sim 95\%$ at 537 nm (green light) and $\sim 88\%$ at 1500 nm (IR light). The current–voltage (*I–V*) measurements were made using a Hewlett Packard 4140 B characterization unit with 10 mA and 100 V max capability. Electroluminescence spectra were collected using an Acton Research spectrometer. Optical power measurements were made using a Newport 1818-SL/CM optical power meter. An MMR Technologies low temperature microprobe system with a K-20 heater controller was used for the temperature studies.

III. Results and Discussion

A schematic cross section of the GaN:Er ELD is shown in Fig. 1. A small circular inner electrode is separated from a much larger outer electrode, which surrounds it. The temperature dependence of the linear *I–V* characteristics for a typical GaN:Er ELD on silicon is also shown in Fig. 1. Notice that the positive and negative bias regions are nearly symmetrical at all temperatures. Visible and IR emission is present under both positive and negative bias, but intensity is greater under the negatively biased electrode. This is most likely due to the fact that there is avalanche breakdown occurring under the electrode, as discussed in detail later. There is almost no emission from the inter-electrode region. The efficiency of the light emission process changes as a function of temperature and will also be described later.

At room temperature (300 K) the device shows a low current regime until a bias of $\sim$ 70 V is reached, after which significant current flow ensues. We will show that this is actually the breakdown voltage of the reverse biased diode. The breakdown voltage decreases with increasing temperature, which has been shown to be related to the presence of defects [23] in similar material.

The choice of ITO as both the emitting and ground contact was made for reasons of convenience. Using ITO for both electrodes allowed for single mask device patterning. An additional advantage of using ITO is that it is semitransparent in both the visible and infrared wavelengths. The conductivity of the ITO is also nearly independent of temperature. ITO has been used as a contact for both n-type [24] and p-type [25] GaN. However, GaN:Er is basically semi-insulating and we consider ITO to be a Schottky contact.

Previously, we reported aluminum contact devices [19] that showed diode like behavior. Further investigation of the devices has led to the development of a device model that more accurately describes the *I–V* characteristic. Since there is no model for carrier transport in GaN:Er specifically, we also present a

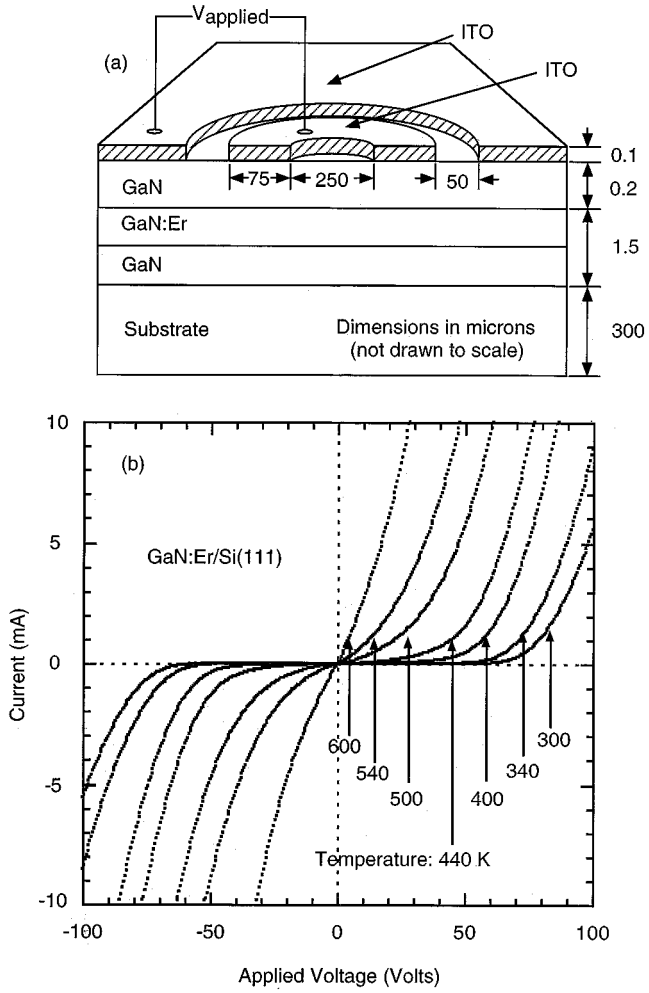

Fig. 1. GaN:Er electroluminescent device: (a) Structural diagram; (b) *I–V* dependence of a GaN:Er ELD on silicon for temperatures from 300 to 600 K.

simple carrier transport model of the material based on the temperature dependence of the *I–V* measurements. As a starting point, we have narrowed the current controlling factors down to two:

a) the ITO/GaN contacts;
b) the GaN film conductivity.

Fig. 2(a) shows a simple equivalent circuit model of our devices on sapphire. The key point is that no matter what bias polarity is applied, one Schottky diode is forward biased and one Schottky diode is reverse biased. It is the reverse biased diode that controls the flow of current initially. No current flows until a significant voltage is reached, at which point the reverse biased diode undergoes avalanche breakdown. Current begins to flow through the forward biased diode. At this point, the resistor in between the two diodes, representing the GaN:Er film, becomes important. Fig. 2(b) is the equivalent circuit model for devices on Si. It is essentially the same with the addition of carrier flow across the GaN/Si junction. Notice that if charge flows through the lateral GaN resistor and through the Si, then the model can be viewed as that seen in Fig. 2(a), except the resistor becomes the series resistance of the entire device. The carrier transport of the resistor is somewhat complicated and is considered in more detail later.

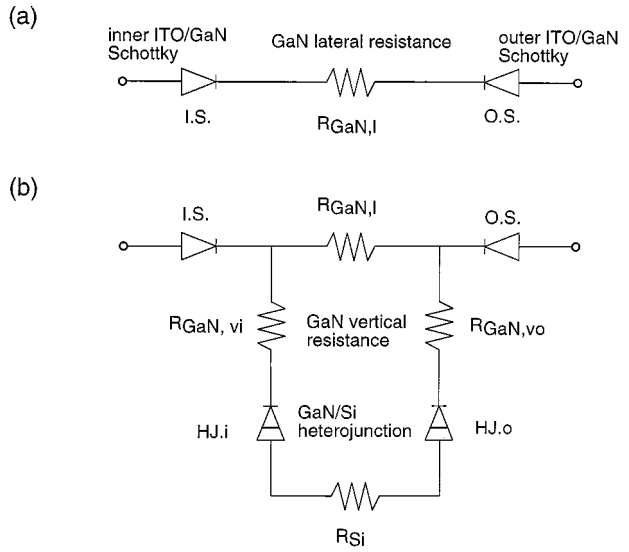

Fig. 2. Equivalent circuit diagrams of ELDs on: (a) sapphire and (b) silicon.

Current through the ITO/GaN contacts is likely to be thermally activated according to the thermionic emission relation:

$$J = A^{**}T^2 \exp\left(\frac{-q\Phi_{bn}}{k_B T}\right)\left[\exp\left(\frac{qV}{k_B T}\right) - 1\right] \qquad (1)$$

where J is the current density in $\mathrm{A/cm^2}$, A^{**} is the effective Richardson's constant, T is temperature in Kelvins, q is the charge of an electron, $\Phi_b n$ is the Schottky barrier height, k_B is Boltzmann's constant and V is the applied bias in volts. Significant current does not flow until the reverse biased diode breaks down. After that, the current is controlled by the forward biased diode along with the series resistance of the device.

With this in mind, the effects of substrate type and erbium doping on current transport were investigated as a function of temperature. The results are summarized in Fig. 3. In general, photoemissive GaN:Er films are quite resistive with 100 V applied bias resulting in 1 to 50 mA of current. In order to understand the role that erbium doping plays in the current conduction mechanism, devices were fabricated on undoped and erbium-doped GaN films grown on sapphire under similar growth conditions [Fig. 3(a) and 3(b)]. The use of insulating sapphire is helpful in determining current transport mechanisms because it prevents current flow through the substrate. It is therefore assumed that all current flow is through the GaN:Er layer in Fig. 3(a) and 3(b). For comparison, the temperature dependence of the current flow of a GaN:Er ELD formed on a Si substrate is shown in Fig. 3(c). Since all graphs shown in Figs. 3(a) to 3(c) use the same scale, it is instructive to comment on the slopes which indicate an electron emission mechanism [26].

Fig. 3(a) shows the effect of erbium doping on carrier generation. The device current is plotted versus inverse temperature. Samples #164 and #162 are both undoped GaN, while sample #107 is doped with erbium. All three samples were biased with a constant voltage of 1 V. In this case, breakdown has not occurred, and the current measured is the reverse saturation current described in (1) and the ohmic current of the GaN:Er resistor. Fig. 3(a) shows that the slopes of the I-T curves for all three samples are similar for temperatures below ~ 25 °C. However,

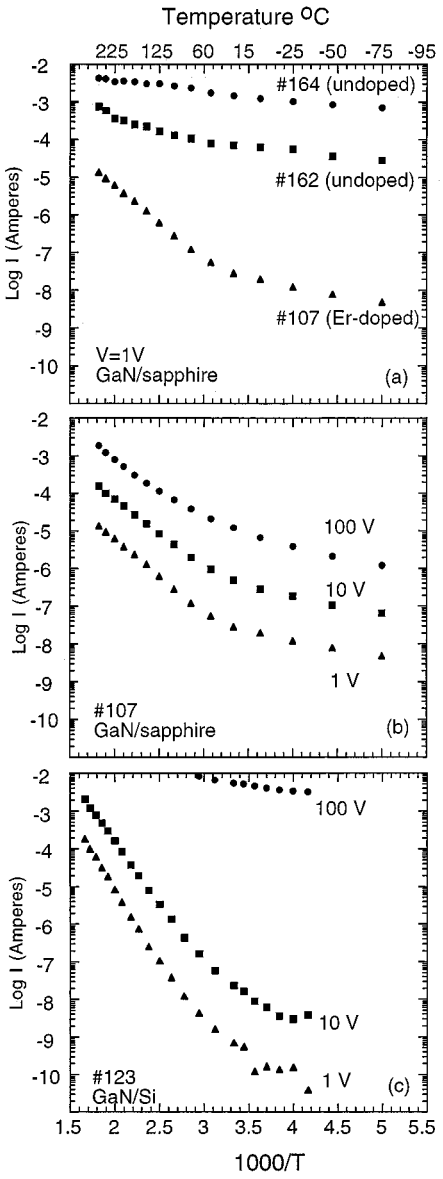

Fig. 3. Current as a function of temperature for devices fabricated and operated under the following conditions: (a) Er-doped and undoped GaN on sapphire, 1 V applied bias; (b) GaN:Er on sapphire at 1, 10, 100 V bias; (c) GaN:Er on Si at 1, 10, 100 V bias.

the Er-doped sample (#107) shows a second distinct I-T slope for temperatures greater than 25 °C. This suggests that the activation mechanism for undoped GaN is also present in Er-doped GaN at low temperature, but that the presence of erbium changes the electron emission mechanism. We model this situation as Frenkel-Poole emission [26] wherein electrons are trapped by an erbium related defect:

$$J \sim \varepsilon \exp\left[\frac{-q\left(\Phi_B - \left(\frac{q\varepsilon}{\pi \in_i}\right)^{1/2}\right)}{k_B T}\right] \qquad (2)$$

where ϵ is the electric field Φ_B is the trap barrier and height $\in_{\mathrm{I}}$ is the insulator dynamic permittivity.

The distinct changes in slope of the erbium doped ELDs (#107, 123) indicate that Frenkel-Poole emission becomes the

dominant conduction mechanism at temperatures above 25 °C. Below 25 °C the current is controlled by thermionic emission across the junction. The final point of interest in Fig. 3(a) is the overall conductivity of each sample. Although the two undoped samples shown here are more conductive than the erbium-doped sample, this is not always the case and depends strongly on growth parameters, especially the gallium flux used during MBE growth of the material.

Fig. 3(b) shows the behavior of a GaN:Er device fabricated on sapphire (#107) at bias voltages of 1, 10, and 100 V. The device biased at 1 V is not in breakdown at most temperatures, while the device biased at 100 V is in breakdown at most temperatures. The fact that the slopes of the I-T characteristics are independent of voltage indicates that electron emission mechanisms are not affected by the breakdown occurring in the reverse biased junction. As in Fig. 3(a), the dominant electron emission mechanism changes around room temperature. Although the device becomes more conductive at higher voltage, the log I versus 1/T slopes do not change, indicating that the carrier generation mechanism is still the same. The fact that a $\sim$ 10 X increase in voltage results in a $\sim$ 10 X increase in current simply indicates that the resistance of the devices (on sapphire) is not a function of voltage. This is not the case for devices using silicon as the substrate.

Fig. 3(c) shows the behavior of an erbium doped GaN ELD fabricated on **silicon** under bias conditions of 1, 10, and 100 V. For bias voltages of 1 and 10 V, the I-T dependence is very similar to that of the ELD on sapphire shown in Fig. 3(b). However, when the device fabricated on silicon is biased at 100 V, the resistance of the device drops dramatically. This indicates that current flows across the GaN/Si heterojunction. We suggest that this causes the device series resistance to decrease by allowing current to flow through the Si substrate, which is more conductive than the GaN:Er film.

Figs. 4 and 5 show photographs of devices during EL operation. Fig. 4 shows devices on Si. The same structure as in Fig. 1(a) still applies, but instead of using the large electrode which surrounds ring A as a bias point, a second ring electrode (B) was used to eliminate the effect of electrode size, by keeping them equal. The two equal area electrodes both emit, but the negative-biased electrode is always brighter. This suggests that the most important factor in generating light emission in these devices is the electric field intensity, which is highest in the reverse biased junction [see Fig. 2(a)]. Fig. 5 shows devices fabricated on sapphire during EL operation. The inner dashed white circle has been added to outline the ring electrode. Here, the bias scheme is identical to that shown in Fig. 1(a). Current crowding is likely occurring at the edges of the electrodes. In this case, it is clear that current density is also important in the light emission process. The ring electrode is negative in Fig. 5(a), and positive in Fig. 5(b). Notice that negative bias produces more emission when applied to either the inner or outer electrode.

This evidence supports the idea that impact excitation is the dominant electroluminescence mechanism. The emission uniformity under the electrodes of devices on silicon versus sapphire confirms that carriers flow through the silicon for devices on silicon, and current crowding is taking place in devices on sapphire.

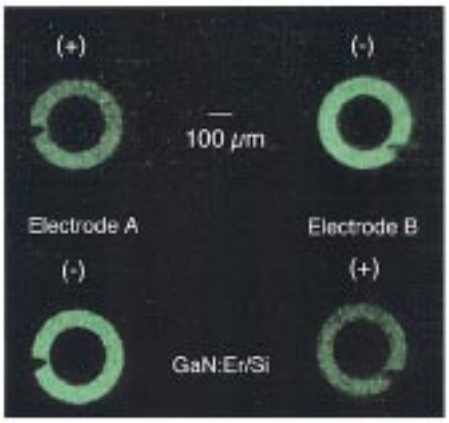

Fig. 4. Photographs of green emission during EL operation of devices fabricated on Si. Two ring electrodes of the same area (A and B) are alternately biased positive and negative.

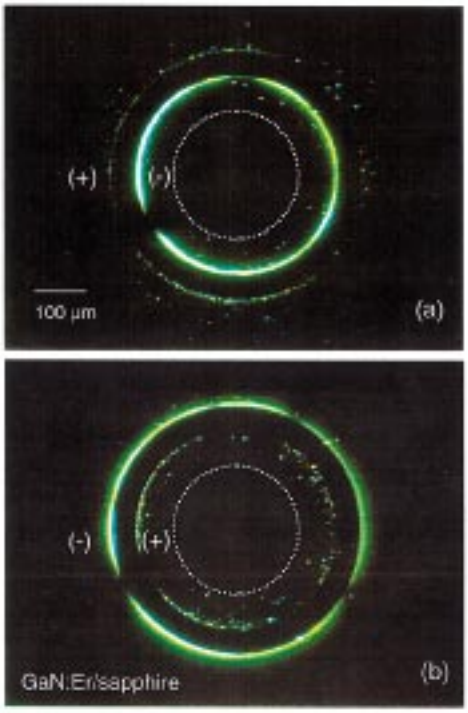

Fig. 5. Photographs of green emission during EL operation of devices fabricated on sapphire: (a) inner electrode—negatively biased; (b) inner electrode—positively biased. In both cases, 250 V applied bias results in 0.44 mA current.

Fig. 6–11 contain electroluminescence data from GaN:Er ELDs fabricated on silicon. The erbium concentration for these samples was kept constant at a value of approximately 6×10^{20} cm^{-3}, as determined by secondary ion mass spectroscopy (SIMS). The effect of erbium doping concentration on the luminescence intensity was recently reported by Lee *et al.* [27]. Fig. 6 shows the temperature dependence of the visible EL emission spectrum. The power applied to the device was kept constant at 250 mW. In addition to the previously identified transitions at 537 and 558 nm, a peak at 666 nm is attributed to the $^4F_{9/2} - {}^4I_{15/2}$ transition. Notice that there is no appreciable shift in wavelength of the light emitted, but that the intensity of the light emitted at each wavelength varies with temperature. The 537-nm line and the 558-nm line (both green) seem to be

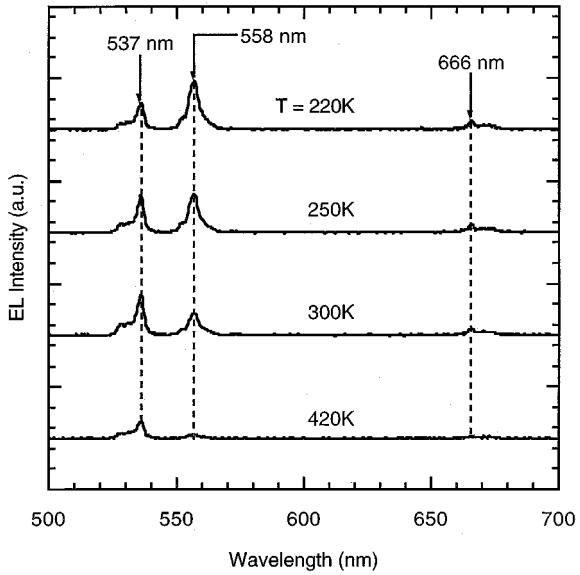

Fig. 6. Visible EL spectrum as a function of temperature.

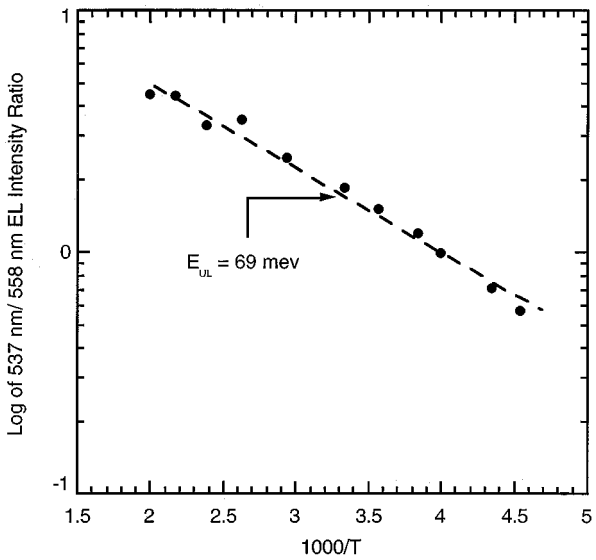

Fig. 8. Determination of the energy gap between the 537-nm and 558-nm lines.

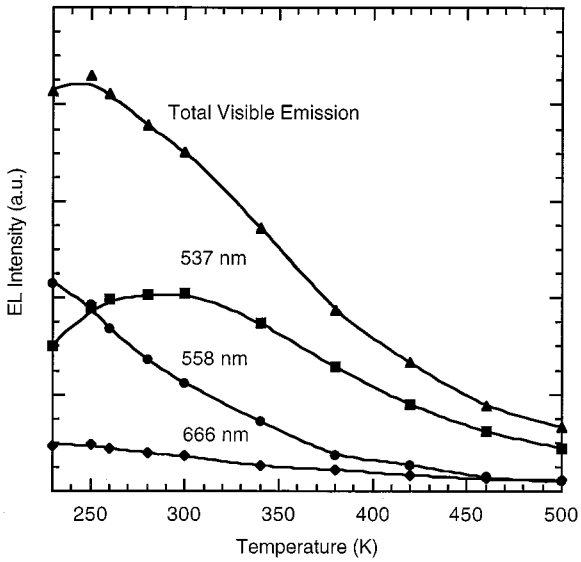

Fig. 7. Peak intensity of the 537-nm and 558-nm lines as a function of temperature.

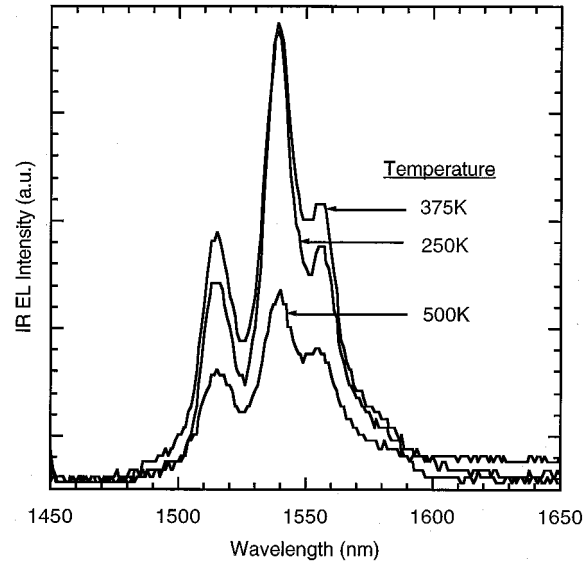

Fig. 9. GaN:Er IR ELD spectrum at three operating temperatures: 250, 375, and 500 K.

coupled, whereas the 666-nm line (red) simply decreases in intensity as temperature is increased.

Fig. 7 shows the temperature dependence of the EL peak intensity of the individual visible emission lines shown in Fig. 6. It clearly shows that each Er^{3+} electronic transition is excited differently as the temperature is varied. We observe that electrical pumping induces the same temperature dependence first reported through the use of optical pumping [15]. Therefore, we can conclude that the temperature dependence of the visible emission intensity is solely a function of temperature and not the pumping method.

The effect of thermalization is shown in Fig. 8, which can be used to calculate the difference in energy between the 537 and 558 nm lines using the relation:

$$\frac{I_u}{I_l} = A\exp\left(\frac{-E_u}{k_B T}\right) \tag{3}$$

where I_u and I_l are the luminescence intensities of the upper and lower levels, $E_{\rm ul}$ is the energy difference between the two levels and A is a constant containing the degeneracy and spontaneous emission rates of the two levels. The $E_{\rm ul}$ calculated from these data is 69 meV, which is lower than the value of 87 meV calculated using the difference in wavelength between the two EL peaks. Interestingly, the same calculation using PL data[16] from similar GaN:Er samples results in a value for $E_{\rm ul}$ of 101.5 meV. The PL method overestimates the energy difference by 14.5 meV, whereas the EL method underestimates the value by 18 meV. This suggests that thermalized electrons transition to the ground state from different energy sublevels of the 537 and 558 nm states depending on whether optical or electrical pumping is used. This information may be useful when considering optical amplification and laser applications for this material.

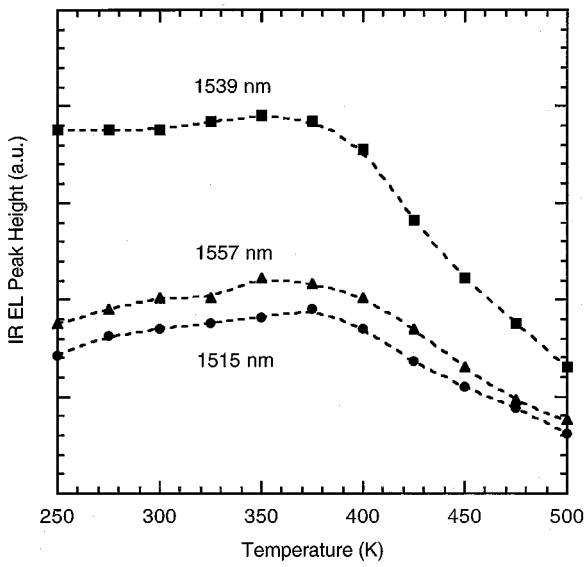

Fig. 10. EL intensity of the three main IR peaks: 1515, 1537, 1558 nm.

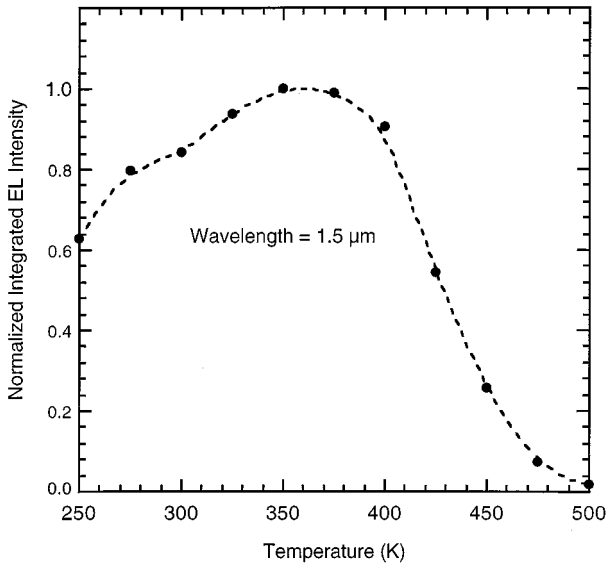

Fig. 11. Normalized integrated EL intensity of the 1.5 μm emission.

In addition to exploring the temperature behavior of the green transitions observed in GaN:Er ELD operation, the temperature behavior of the 1.5 μm IR emission was also investigated. Fig. 9 shows the IR spectrum as a function of temperature. Three distinct peaks at 1515, 1537, and 1558 nm are observed. The spectrum with highest peak intensity is at 375 K. Fig. 10 shows the peak intensity of the three different IR peaks heights (clustered around 1.5 μm) as a function of temperature. This graph illustrates that the individual peaks have essentially the same temperature dependence. The IR intensity begins to decrease at temperatures of 375 to 400 K.

The temperature dependence of the integrated EL intensity is shown in Fig. 11. Notice that the intensity actually peaks at around 375 K. This is very important for 1.5 μm erbium devices operating at or near room temperature, especially when considering the temperature quenching of the IR light in other semiconductor hosts. GaN shows superior IR temperature performance compared to GaAs, GaP and Si, which have been studied for Er-based light emitting applications. Notice that at least 90% of the maximum value is obtained for operating temperatures in the range from 270 K to 410 K.

IV. Summary and Conclusion

In summary, we have reported on the temperature dependence of visible and IR rare-earth-activated electroluminescence of Er-doped GaN. We showed that a simple model consisting of two back-to-back Schottky diodes accurately describes the *I-V* relationship. We have found that current transport is controlled by an Er-related electron trap at temperatures above 300 K and by an intrinsic carrier mechanism of the GaN at temperatures below 300 K. The substrate conductivity was seen to greatly affect the measured current. Spatial confinement of the emission during EL operation was explained in terms of emission intensity as a function of bias polarity and substrate type, based on the device model. Current density and electric field are both important in determining the location and intensity of light emission. The fact that the 537-nm peak is at highest intensity at 300 K and does not shift in wavelength at any reasonable temperature indicates that GaN:Er green light emitters can find practical applications. Light emitting devices based on erbium doped GaN will utilize either silicon or sapphire substrates depending on the application. For example, the use of silicon substrates would be attractive for flat panel display applications using visible emission from erbium doped GaN. For IR (1.5 μm) telecommunication applications, the use of the sapphire substrate, with its low refractive index would be desirable.

Acknowledgment

The authors would like to thank D.S. Lee and J. Heikenfeld for many useful discussions on the operation of GaN:Er devices and R. Paugh at MMR Technologies for his technical support. The authors are also pleased to acknowledge the support of M. Gerhold, N. El-Masry, and J. Zavada.

References

[1] D. Kahng, "Electroluminescence of rare-earth and transition metal molecules in II-VI compounds via impact excitation," *Appl. Phys. Lett.*, vol. 13, pp. 210–212, 1968.

[2] N. Miura, K. Ogawa, S. Kobayashi, H. Matsumoto, and R. Nakano, "Electroluminescence spectra of rare-earth doped $ZnS_{1-x}Se_x$ thin films," *J. Cryst. Growth*, vol. 138, pp. 1046–1050, 1994.

[3] G. Harkonen, M. Leppanen, E. Soininen, R. Tornqvist, and J. Viljanen, "Multicolor thin film electroluminescence displays: a new application of rare earth metals," *J. Alloys Compounds*, vol. 225, pp. 552–554, 1995.

[4] A. M. Emel'yanov, N. A. Sobolev, and A. N. Yakimenko, "Anomalous temperature dependence of erbium-related electroluminescence in reverse biased silicon p-n junction," *Appl. Phys. Lett.*, vol. 72, pp. 1223–1225, 1998.

[5] C. Du, W. Ni, K. B. Joelsson, and G. V. Hansson, "Room temperature 1.54 μm light emission of erbium doped Si Schottky diodes prepared by molecular beam epitaxy," *Appl. Phys. Lett.*, vol. 71, pp. 1023–1025, 1997.

[6] A. Reittinger, J. Stimmer, and G. Abstreiter, "Influence of the erbium and oxygen content on the electroluminescence of epitaxially grown erbium-doped silicon diodes," *Appl. Phys. Lett.*, vol. 70, pp. 2431–2433, 1997.

[7] J. Stimmer, A. Reittinger, J. F. Nutzel, and G. Abstreiter, "Electroluminescence of erbium-oxygen-doped silicon diodes grown by molecular beam epitaxy," *Appl. Phys. Lett.*, vol. 68, pp. 3290–3292, 1996.

[8] Y. H. Xie, E. A. Fitzgerald, and Y. J. Mii, "Evaluation of erbium-doped silicon for optoelectronic evaluations," *J. Appl. Phys*, vol. 70, pp. 3223–3228, 1991.
[9] G. M. Ford and B. W. Wessels, "Electroluminescence from forward-biased Er-doped GaP p-n junctions at room temperature," *Appl. Phys. Lett.*, vol. 68, pp. 1126–1128, 1996.
[10] P. N. Favennec, H. L'Haridon, M. Salvi, D. Moutonnet, and Y. LeGuillou, "Luminescence of erbium implanted in various semiconductors: IV, III-V and II-VI materials," *Electron. Lett.*, vol. 25, pp. 718–719, 1989.
[11] J. T. Torvik, C. H. Qiu, R. J. Feuerstein, J. I. Pankove, and F. Namavar, "Photo-, cathodo-, and electroluminescence from erbium and oxygen co-implanted GaN," *J. Appl. Phys.*, vol. 81, pp. 6343–6350, 1997.
[12] C. H. Qiu, M. W. Leksono, J. I. Pankove, J. T. Torvik, R. J. Feuerstein, and F. Namavar, "Cathodoluminescence study of erbium and oxygen coimplanted gallium nitride thin films on sapphire substrates," *Appl. Phys. Lett.*, vol. 66, pp. 562–564, 1995.
[13] M. Thaik, U. Hommerich, R. N. Schwartz, R. G. Wilson, and J. M. Zavada, "Photoluminescence spectroscopy of erbium implanted gallium nitride," *Appl. Phys. Lett.*, vol. 71, pp. 2641–2643, 1997.
[14] S. Kim, S. J. Rhee, D. A. Turnbull, X. Li, J. J. Coleman, S. G. Bishop, and P. B. Klein, "Trap-mediated excitation of Er^{3+} photoluminescence in Er-implanted GaN," *Appl. Phys. Lett.*, vol. 71, pp. 2662–2664, 1997.
[15] A. J. Steckl and R. Birkhahn, "Visible emission from Er-doped GaN grown by solid source molecular beam epitaxy," *Appl. Phys. Lett.*, vol. 73, pp. 1700–1702, 1998.
[16] R. Birkhahn and A. J. Steckl, "Green emission from Er-doped GaN grown by molecular beam epitaxy on Si substrates," *Appl. Phys. Lett.*, vol. 73, pp. 2143–2145, 1998.
[17] H. J. Lozykowski, W. M. Jadwisienczak, and I. Brown, "Visible cathodoluminescence of GaN doped with Dy, Er, and Tm," *Appl. Phys. Lett.*, vol. 74, pp. 1129–1131, 1999.
[18] A. J. Steckl, M. Garter, and R. B. Scofield, "Green electroluminescence from Er-doped GaN Schottky barrier diodes," *Appl. Phys. Lett.*, vol. 73, pp. 2450–2452, 1998.
[19] M. Garter, J. Scofield, R. Birkhahn, and A. J. Steckl, "Visible and infrared rare-earth activated electroluminescence from indium tin oxide Schottky diodes to GaN:Er on Si," *Appl. Phys. Lett.*, vol. 74, pp. 182–184, 1999.
[20] M. Garter, R. Birkhahn, A. J. Steckl, and J. Scofield, "Visible and infrared rare-earth activated electroluminescence from erbium doped GaN," *MRS Internet J. Nitride Semicond. Res. 4S1, G11.3*, 1999.
[21] R. Birkhahn, R. Hudgins, D. Lee, A. J. Steckl, R. J. Molnar, A. Saleh, and J. M. Zavada, "Growth and morphology of er-doped gan on sapphire and hydride vapor phase epitaxy substrates," *J. Vac. Sci. Technol. B*, vol. 17, pp. 1195–1199, 1999.
[22] R. Birkhahn, R. Hudgins, D. S. Lee, B. K. Lee, A. J. Steckl, A. Saleh, R. G. Wilson, and J. M. Zavada, "Optical and structural properties of Er-doped GaN grown by MBE," *MRS Internet J. Nitride Semicond. Res. 4S1, G3.80*, 1999.
[23] R. Raghunathan and B. J. Baliga, "Role of defects in producing negative temperature dependence of breakdown voltage in SiC," *Appl. Phys. Lett.*, vol. 72, pp. 3196–3198, 1998.
[24] J. K. Sheu, Y. K. Su, G. C. Chi, M. J. Jou, and C. M. Chang, "Effects of annealing on the indium tin oxide Schottky contacts of n-GaN," *Appl. Phys. Lett.*, vol. 72, pp. 3317–3319, 1998.
[25] T. Margalith, O. Buchinsky, D. A. Cohen, A. C. Abare, M. Hansen, S. P. DenBaars, and L. A. Coldren, "Indium tin oxide contacts to gallium nitride optoelectronic devices," *Appl. Phys. Lett.*, vol. 74, pp. 3930–3932, 1999.
[26] S. M. Sze, *Physics of Semiconductor Devices*. New York: Wiley, 1981, pp. 402–7.
[27] D. S. Lee, J. Heikenfeld, A. J. Steckl Hommerich, J. T. Seo, A. Braud, and J. Zavada, "Optimum Er concentration for in situ doped GaN visible and infrared luminescence," *Appl. Phys. Lett.*, vol. 79, pp. 719–721, 2001.

Michael J. Garter received the B.S. degree in electrical engineering in 1996 and the Ph.D. degree in 2001 from the University of Cincinnati, Cincinnati, OH. His undergraduate research led to the fabrication of silicon micromirrors using MEMS techniques.

In 1996, he joined the Nanoelectronics Laboratory at the University of Cincinnati. During his first two years, he focused on plasma etching of SiC and GaN. His focus then shifted to the MBE growth, fabrication, and testing of erbium doped GaN electroluminescent devices. During his graduate work, he gave several formal presentations, including a paper at the Device Research Conference in June, 1999. His graduate research has also resulted in the publication of over ten papers and a U.S. patent on rare-earth doped GaN electroluminescence. He is currently employed at CMC Electronics Cincinnati, Mason, OH where he works on the fabrication and optimization of infrared light detection products.

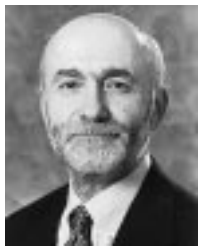

Andrew J. Steckl (S'70–M'73–SM'79–F'99) received the B.S.E. degree in electrical engineering from Princeton University, Princeton, NJ, in 1968, and the M.Sc. and Ph.D. Degrees from the University of Rochester, Rochester, NY, in 1970 and 1973, respectively.

In 1972, he joined the Honeywell Radiation Center, Lexington, MA, as a Senior Research Engineer, where he worked on new concepts and devices in the area of infrared detection. In 1973, he joined the Technical Staff of the Electronics Research Division of Rockwell International, Anaheim, CA. At Rockwell he was primarily involved in research on charge coupled devices. In 1976, he joined the Electrical, Computer and Systems Engineering Department at Rensselaer Polytechnic Institute, Troy, NY, where he developed a research program in microfabrication of Si devices. In 1981, he founded the Center for Integrated Electronics, a multi-disciplinary academic center focused on VLSI research and teaching, and served as its director until 1986. In 1988, he joined the Electrical and Computer Engineering Department of the University of Cincinnati as Ohio Eminent Scholar and Gieringer Professor of Solid State Microelectronics. At Cincinnati he has built the Nanoelectronics Laboratory with research activities in semiconductor materials and devices for photonics: SiC and GaN thin-film growth by CVD and MBE, focused ion beam fabrication of photonic components and circuits, rare-earth-doped luminescent devices for flat panel displays, and communications. His research has resulted in 280 publications and over 300 conferences and seminar presentations.